Andean Geology 42 (1): 20-35. January, 2015
doi: 10.5027/andgeoV42n1-a02

Andean Geology
www.andeangeology.cl

Neogene structure of the Andean Precordillera, Argentina: insights from analogue models

***Sebastián Oriolo[1], Ernesto O. Cristallini[2], María S. Japas[3], Daniel L. Yagupsky[2]**

[1] *Departamento de Ciencias Geológicas, Universidad de Buenos Aires, Intendente Güiraldes 2160, Buenos Aires, Argentina. seba.oriolo@gmail.com*
[2] *Laboratorio de Modelado Geológico, IDEAN (UBA-CONICET), Intendente Güiraldes 2160, Buenos Aires, Argentina. ernesto@gl.fcen.uba.ar; daniely@gl.fcen.uba.ar*
[3] *Instituto de Geociencias Básicas, Aplicadas y Ambientales (CONICET-UBA), Intendente Güiraldes 2160, Buenos Aires, Argentina. msjapas@gl.fcen.uba.ar*

* *Corresponding author: seba.oriolo@gmail.com*

ABSTRACT. Analogue models combining different sets of preexisting structural weaknesses were developed to understand their evolution during regional ~ENE shortening. Strain analysis of simulations was performed with the GEODEF 1.1 software, a tool that allows to quantify deformation in plan view on the basis of displacement fields. Results showed up that regional NNE heterogeneities are reactivated as dextral reverse-slip structures, though NNE neoformed thrusts are also present. Likewise, dominant sinistral strike-slip motions have been obtained for reactivated second-order WNW structures whereas sinistral reverse-slip has been recorded for NW ones. Comparison of these results with structural, kinematic and paleomagnetic data supports partitioned dextral transpression for the northern Andean Precordillera since the Miocene. Moreover, models not only confirm sinistral strike-slip motions for WNW structures of the Precordillera but also suggest that they would represent preexisting crustal fabrics that were reactivated during the Andean orogeny. These cross-strike structures have played a significant role in the construction and evolution of the fold and thrust belt as they segmentate the activity of orogen-parallel structures.

Keywords: Transpression, Cross-strike structures, Strain partitioning, Inherited crustal fabrics, Flat-slab subduction, GEODEF software.

RESUMEN. Estructura neógena de la Precordillera Andina, Argentina: aportes de modelos análogos. Se llevaron a cabo una serie de modelos análogos en los que se combinaron diferentes sistemas de debilidades estructurales preexistentes a fin de entender su evolución vinculada a acortamiento regional en dirección ~ENE. El análisis de la deformación de las simulaciones fue realizado a través del software GEODEF 1.1, una herramienta que permite la cuantificación de la deformación en planta sobre la base de campos de desplazamiento. Los resultados obtenidos muestran que las heterogeneidades regionales de rumbo NNE se reactivan como estructuras dextrales inversas, si bien también se generan corrimientos neoformados de igual orientación. Asimismo, se obtuvieron desplazamientos de rumbo sinistral dominante para estructuras reactivadas de segundo orden de rumbo WNW, mientras que desplazamientos sinistrales inversos se registraron en aquellas de rumbo NW. La comparación de estos resultados con datos estructurales, cinemáticos y paleomagnéticos señala la existencia de transpresión dextral particionada para el precordillera norte desde el Mioceno. A su vez, los modelos no solo confirman los desplazamientos de rumbo sinistral para las estructuras WNW de la precordillera, sino que también sugieren que estas constituirían fábricas corticales preexistentes que fueron reactivadas durante la orogenia andina. Estas estructuras oblicuas han tenido un rol significativo en la construcción y evolución de la faja plegada y corrida, ya que segmentan la actividad de las estructuras paralelas al orógeno.

Palabras clave: Transpresión, Estructuras oblicuas, Partición de la deformación, Fábricas corticales heredadas, Subducción plana, programa GEODEF.

1. Introduction

The Precordillera represents an almost north-trending morphostructural unit that was developed within the Andean foreland due to flat-slab subduction in the Pampean segment (Fig. 1; Ramos, 1999a; Ramos *et al*., 2002). This process is related to the subduction of the Juan Fernández Ridge between 28º and 33ºS since Miocene times and gives rise to the migration of deformation and arc magmatism into the foreland (Pilger, 1984; Kay *et al*., 1987; Allmendinger *et al.,* 1990; Jordan *et al*., 1993; Ramos, 1999a).

The Andean Precordillera can be divided into two segments: northern and southern. The northern Precordillera comprises a NNE-trending fold and thrust belt (Allmendinger *et al*., 1990; Cristallini and Ramos, 2000) while the southern Precordillera evolved as a consequence of the reactivation of NNW to NNE Paleozoic-Triassic structures (Cortés *et al*., 2005, 2006; Giambiagi *et al*., 2010). However, the tectonic evolution of the northern Precordillera is still controversial as different models have been proposed. The fold and thrust belt was defined by Allmendinger *et al*. (1990) and Cristallini and Ramos (2000), whereas Ré *et al*. (2001), Siame *et al*. (2005) and Álvarez Marrón *et al*. (2006) considered dextral transpression for the Andean deformation of the Precordillera.

WNW structures have been also described within the northern Precordillera. They were first suggested by Japas (1998), Ré *et al*. (2000, 2001), Japas *et al*. (2002a, b) and Ré and Japas (2004) and then confirmed as sinistral cross-strike structures in the Hualilán region (Oriolo, 2012; Oriolo *et al*., 2013). These authors have considered these cross-strike structures as reactivated pre-Neogene fabrics, though a possible Miocene age can not be discarded.

The aim of this paper is to understand the structural evolution of the northern Precordillera on the basis of analogue models considering the role and interaction of major NNE structures and subordinated WNW cross-strike structures. These models have been interpreted with the software GEODEF 1.1 (Yagupsky, 2010) which let to quantify both incremental and finite strain. Consequently, the Andean deformation of the Precordillera is constrained by a comparative analysis between deformation patterns in models and geological data.

2. Geological setting

2.1. Regional framework

The northern Precordillera is located in the Andean foreland between the Frontal Cordillera to the west and the Sierras Pampeanas to the east (Fig. 1). It represents a fold and thrust belt that can be divided into three segments (Western, Central and Eastern) with distinctive structural and geological features (Ramos, 1999b and references therein). Western and Central Precordillera represent an east-verging thin-skinned fold and thrust belt, whereas the Eastern Precordillera shows west-verging thick-skinned deformation which is related to the Sierras Pampeanas structure (Fig. 2). Consequently, a thick-skinned triangle zone is developed between both belts (Zapata and Allmendinger, 1996).

Many authors have proposed different hypothesis concerning the Cenozoic tectonic evolution of the Precordillera. The first proposals considered the Precordillera as a fold and thrust belt that developed mostly during the Miocene due to nearly E-W shortening (Allmendinger *et al*., 1990; Cristallini and Ramos, 2000). Later, Siame *et al*. (2005) suggested that the slightly oblique convergence between Nazca and South American plates gives rise to dextral transpression related to a compressive regime. According to these authors, Plio-Quaternary deformations are partitioned between thrusting in the Eastern Precordillera and the Western Sierras

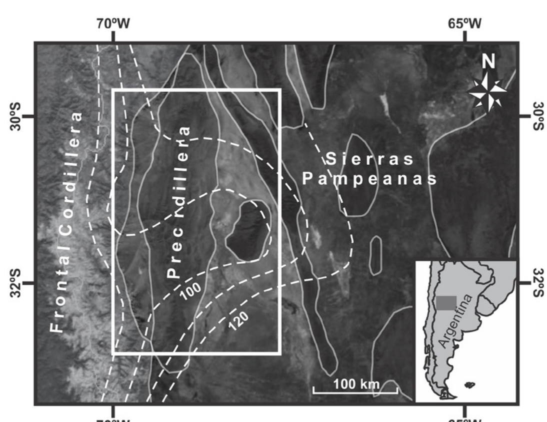

FIG. 1. Location of the Pampean flat-slab segment of the Central Andes. Contours of depth (km) of the oceanic slab (after Anderson *et al*., 2007) and main morphostructural units are shown. Area from figure 2 is indicated.

Pampeanas and dextral strike-slip motions in the El Tigre fault (Fig. 2, Bastías *et al*., 1984; Siame *et al*., 1997; Cortés *et al*., 1999). However, Álvarez Marrón *et al*. (2006) proposed that deformation in the Precordillera is the result of dextral transpression that was developed since Neogene times and produced orogen longitudinal extension and orogen perpendicular compression. Likewise, Ré *et al*. (2001) and Japas *et al*. (2002a) have previously suggested a transpressive system between 22º and 33ºS based on tectonic fabric analysis.

2.2. WNW cross-strike structures

Two systems of conjugated megashear zones at the study latitudes have been proposed (Japas, 1998; Ré *et al*., 2000, 2001; Japas *et al*., 2002a, b; Ré and Japas, 2004): left-lateral NNW and right-lateral NNE transpressional sets, and left-lateral WNW and right-lateral ENE transtensional ones. Left-lateral WNW structures have been confirmed within the Hualilán Belt (Fig. 2) by Oriolo (2012) and Oriolo *et al*. (2013). These authors have remarked the role of these WNW and subordinated ENE cross-strike structures as the main structural control of magmatism emplacement due to the into-the-foreland migration associated with the flat-slab process. Kinematics of cross-strike structures shows dominant strike-slip displacements as well as a minor component of extension that would favor the magmatic output and emplacement.

Ré *et al*. (2001), Oriolo (2012) and Oriolo *et al*. (2013) have also proposed the existence of other cross-strike structural belts, that would be equivalent to the one located in the Hualilán region. One of these is placed between Gualcamayo and Jachal localities (~30º S), where Chernicoff and Nash (2002) have demonstrated the relationship between Cenozoic magmatism and associated ore deposits and NW-WNW cross-strike structures.

3. Analogue modeling

3.1. Background

The three-dimensional complexity of transpressive and transtensive systems has favored the use of analogue models for their study. Early works from Cloos (1928) and Riedel (1929) applied to strike-slip deformation were lately followed by contributions

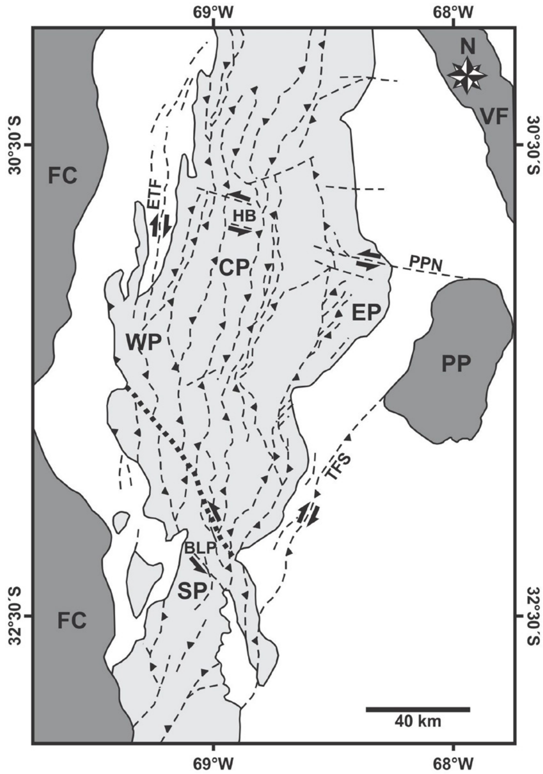

FIG. 2. Structural map of the Precordillera (modified after Cortés *et al*., 2005; Siame *et al*., 2005). **ETF:** El Tigre fault; **HB:** Hualilán belt; **PPN:** Pie de Palo Norte lineament; **TFS:** Tulum fault system; **BLP:** Barreal-Las Peñas belt. Main morphostructural units are indicated: Precordillera (**WP:** Western Precordillera; **CP:** Central Precordillera; **EP:** Eastern Precordillera; **SP:** Southern Precordillera), Frontal Cordillera (**FC**); Sierras Pampeanas (**PP:** Pie de Palo range; **VF:** Valle Fértil range).

related to transpression/transtension (Richard and Cobbold, 1989, 1990; Dooley and McClay, 1997; Rahe *et al*., 1998; Schreurs and Colletta, 1998; Casas *et al*., 2001; among others).

During the last decades, physical models applied to understand strike-slip deformation combined with other geological processes diversified. Richard and Cobbold (1989) and Pinnet and Cobbold (1992) analyzed strain partitioning mechanisms related to transpression due to oblique convergence. Likewise, Le Guerroué and Cobbold (2006) studied the influence of erosion and sedimentation on strike-slip faults, whereas Corti *et al*. (2005), Mathieu and van Wyk de Vries (2011) and Mathieu *et al*. (2011) investigated relationships between transtension/transpression, magmatism and volcanism.

However, analogue models combining different sets of structures with strike-slip displacements are still scarce. Within this framework, this contribution provides information about this interaction and suggests an alternative structural and kinematic model for the Andean foreland system.

3.2. Experimental configuration

Three sandbox analogue experiments (I, II, III) were developed in order to simulate major structural features and their role during the evolution of the northern Precordillera. The models were carried out in a deformation sandbox with dimensions of 70x52x4 cm (Fig. 3), wide enough to avoid boundary effects. Orthogonal compression was applied to a rigid plate A linked to an acetate plate B (Fig. 3). They both were moved towards the right of the model with a velocity of $1x10^{-5}$ m s^{-1} as the shortening increased while an acetate plate C was fixed to the modeling table. A 0.5 cm thick silicone layer was arranged between plates B and C with an angle α=15° between the layer boundary and the plate A, in order to favor the localization of deformation in this area. Within the silicone layer, second-order oblique discontinuities filled with sand were set out in models II and III considering β angles between them and the plate A of 100º and 130º, respectively (Fig. 3). The model was then covered with ~1 cm thick sand layers.

The value of α=15° was selected in order to represent major inherited structures of the Precordillera which have been interpreted as terrane boundaries (*i.e.,* Giménez *et al*., 2008) and are slightly oblique to both directions of convergence of the Nazca plate and regional shortening in the Precordillera (Brooks *et al*., 2003). Subordinated oblique sand ribbons are induced to analyse the influence of pre-existing heterogeneities in the basal level. Their influence during shortening of the overlying sand pile can be compared with cross-strike structures described by Oriolo (2012) and Oriolo *et al.* (2013). Therefore, they were not included in model I in order to determine if they could be developed when they do not represent inherited features.

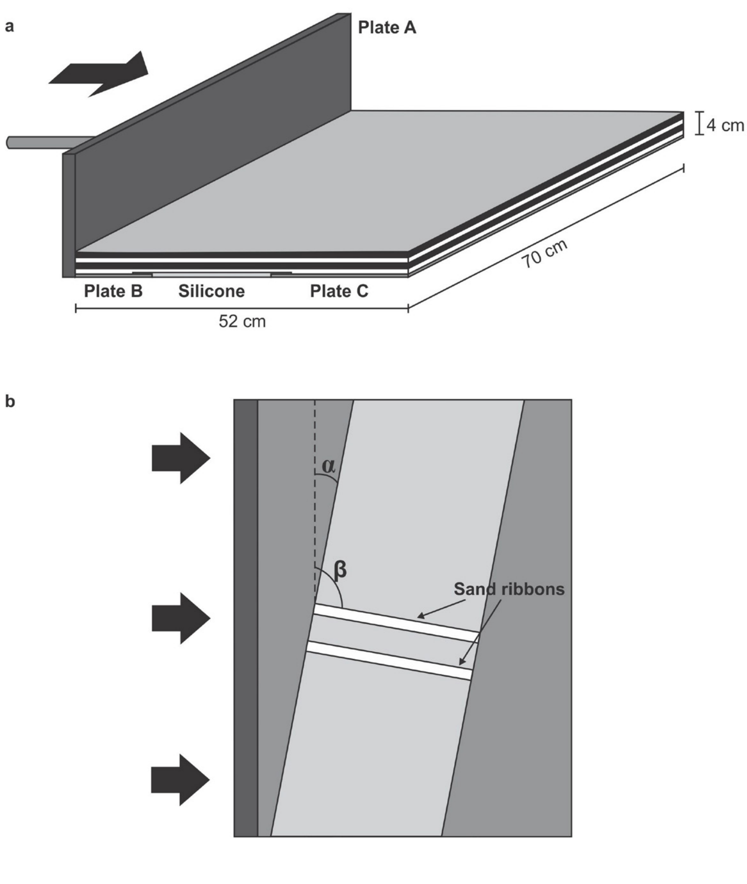

FIG. 3. **a**. Schematic representation of the model setting. Shortening direction is shown (black arrows); **b**. Plan view. The angles between the plate A and the silicone layer (α) and the secondary oblique heterogeneities (β) are indicated.

The analogue materials were well sorted fine-grained dry quartz sand and silicone. The sand has a density ρ=1,400 kg m^{-3}, an internal friction angle φ=32.7° and negligible cohesion C_0<100 Pa (Yagupsky *et al*., 2008) and, therefore, is a good analog for the brittle upper crust (Davy and Cobbold, 1991). The silicone is a viscous material with a viscosity of 2.5x10^3 Pa s (Stewart, 1996, Likerman *et al*., 2013) that can be considered a Maxwell solid (Casassa *et al*., 1986). The selected configuration of sand overlying a silicone layer were used by other authors (Casas *et al*., 2001; Soto *et al*., 2007; Yagupsky *et al*., 2008; Leever *et al*., 2011; Likerman *et al*., 2013), supporting the validity of both set-up and materials.

The comparison between models and natural examples is only possible if the experiments are properly scaled. In this case, a geometric scale factor λ=2x10^{-6} was considered, which represents the ratio between the length of the model and its equivalent length in the nature. Gravity ratio was g´=1, whereas density ratio was ρ´=0.6, considering a mean density ρ=2,500 kg m^{-3} for sedimentary rocks in the Precordillera (Perucca and Ruiz, 2014). Therefore, the stress ratio between models and nature was σ´=ρ´g´λ=1.2x10^{-6}. The shortening rate was V=1x10^{-6} mm y^{-1} and the shortening rate ratio was V´=2x10^{-7}, if an average shortening rate V=5 mm y^{-1} for the last 20 Ma is assumed (Siame *et al*., 2005).

3.3. PIV and GEODEF processing

Photographs in plan view were taken every minute with a camera suspended above the model. These images were then processed using a PIV software (Sveen, 2004), that allows to quantify high-resolution displacement fields between two successive images within the grain-size range (White *et al*., 2001; Adam *et al*., 2005). The software uses an optical correlation to obtain the displacement vectors (Sveen, 2004).

PIV results were reprocessed with the software GEODEF 1.1 (Yaguspky, 2010). GEODEF 1.1 considers the directional derivatives for each incremental vector between two pictures, allowing to calculate the incremental strain matrix for each point of the model. Finite strain for a specific n stage can be estimated as the product of all incremental strain matrices from the first to the n stage (Yagupsky, 2010). This method quantifies the deformation of systems (ellipticities, rotations, strain ellipses) even with extremely low shortening values (~2 mm).

4. Results

4.1. Model I

Model I shows the simplest configuration and, thus, it does not include subordinated oblique heterogeneities. Figure 4 shows results obtained for this configuration.

The resulting structures are mostly thrusts (Fig. 4a-c), which is indicated by the presence of long axes of ellipses parallel to them supporting E-ENE shortening directions (Fig. 4d-f). However, a localized zone with WNW-NW long axes is also present over the western boundary of the silicone plate and it cannot be explained considering only thrusting. Additionally, this zone can be detected only after a certain amount of shortening.

In a first stage, shortening is mainly accommodated in *en-échèlon* structures that resulted from the reactivation of the silicone plate boundaries (Fig. 4a, d, g). The western and eastern structures consist of transpressional structures with respectively W- and E-vergence. *En-échèlon* structures then coalesce, giving rise to a sigmoid pattern (Fig. 4b, e, h). Particularly, the eastern structure shows higher values of ellipticity than the western one. The appearance of neoformed structures contributes to localized shortening, reducing the deformation rate of the early reactivated structures. During the third step, some thrusts developed out from the previously deformed zone bounded by the two main anisotropies, showing variable vergence direction (Fig. 4c).

Although deformation is registered all over the deformed zone placed between the NNE heterogeneities, clockwise rotations seem to be restricted to them (Fig. 4j-l). Areas with higher values of rotations seem to correlate with those with higher values of ellipticity supporting higher values of non-coaxial strain. Low counterclockwise rotation values were only recognized at the final stage of modeling and appear to be linked to the small bends of the NNE-striking structures (Fig. 4l). These bends seem to be related to ENE strike-slip faults that can be interpreted as transfer zones as they segmentate the chain: the northern domain shows deformation concentrated in the fold and thrust belt and its hinterland, and the southern one shows deformation localized in the fold and thrust belt and its foreland.

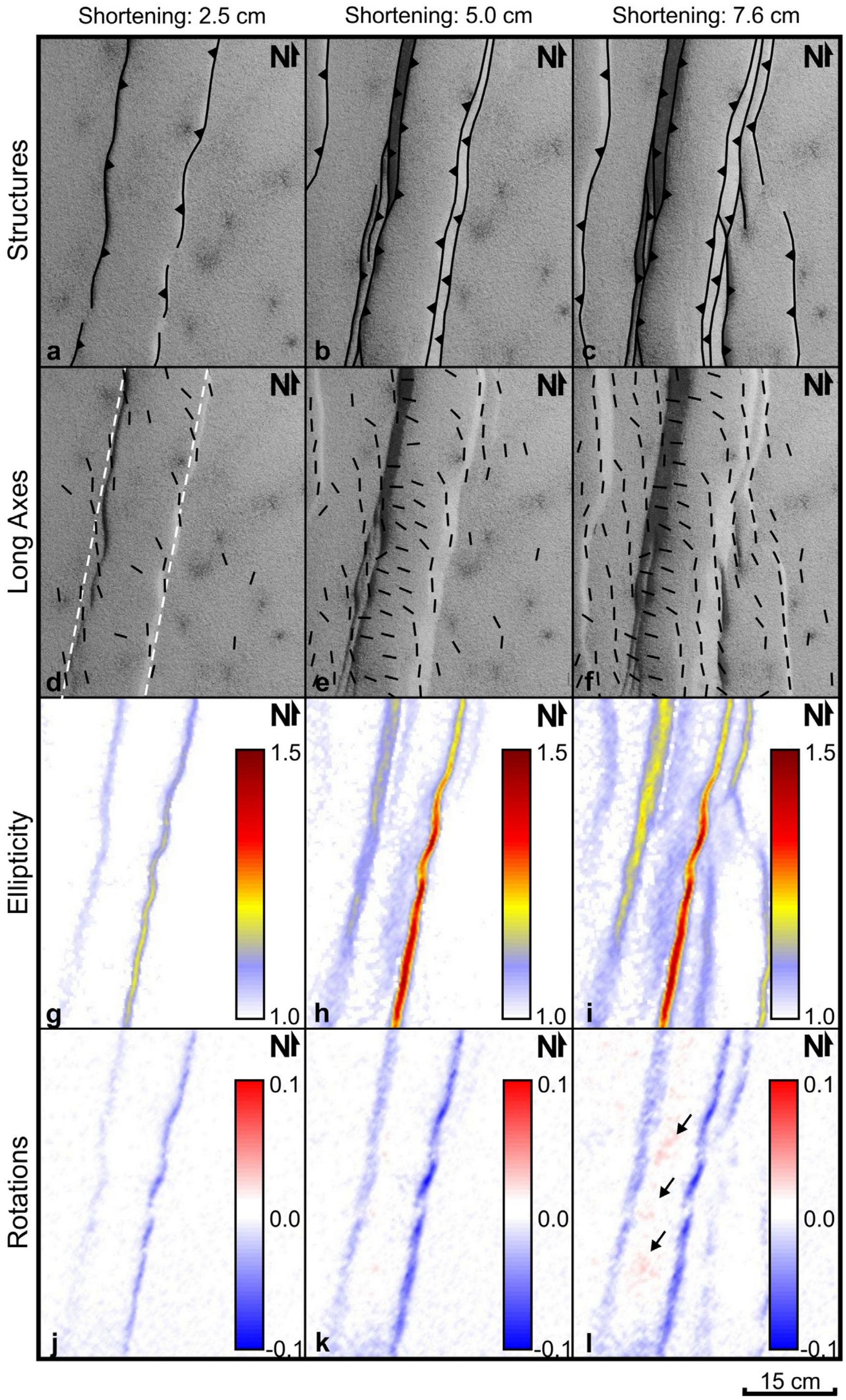

FIG. 4. Deformation stages of model I, considering main structures (**a-c**), long axes of finite strain ellipses (**d-f**), cumulative ellipticity (**g-i**) and cumulative rotations (**j-l**). Values of ellipticity and rotations (negative rotations, clockwise; positive rotations, counterclockwise) are shown in lateral bars. White lines indicate schematic position of anisotropies. Small arrows show areas of local counterclockwise rotations.

4.2. Models II and III

These models consider subordinated oblique discontinuities within the silicone layer. They were set up with two different orientations: β=100º (model II) and β=130º (model III).

Results obtained for model II reveal some similarities with those obtained in model I, as significant E-ENE shortening and localized clockwise rotations are present (Fig. 5). Ellipticity is higher at the backthrust differing with results obtained for model I, where the reactivated eastern heterogeneity has accumulated higher values of ellipticity. Moreover, the higher strain recorded by the western main fault shows two minimums along strike where the two sets of oblique faults are present (Fig. 5l). These localized areas also show deformation migration into the foreland, indicating strong segmentation of the chain by these structures.

WNW faults show neither significant shortening nor extension revealed by cross-sections of the models and very low values of ellipticity but they exhibit localized counterclockwise rotations (Fig. 5n-p). This would reflect dominant strike-slip displacements for these structures. Therefore, it can be interpreted that strain induced by localized pre-existing discontinuities overprints to the previous strain state. Counterclockwise rotations become evident with shortening up to ~3 cm. This would give rise to local sinistral strike-slip displacements that are active in a later step of the model evolution. Scarce thrusts develop in the foreland between WNW faults (Fig. 5d) and each segment of the western NNE fault bounded by these oblique structures grows independently (Fig. 5l). Therefore, these cross-strike structures comprise important deformational features since migration of deformation into the foreland appears to be segmented by them.

Model III evidences shortening and counterclockwise rotations associated with the reactivated oblique structures (Fig. 6). The amount of shortening over them is much higher than that obtained in model II.

NW structures reactivate prior to the development of the main NNE front and shortening is transferred into the foreland by these structures (Fig. 6l). NNE faults are strongly segmented along-strike (Fig. 6l). Therefore, reactivation of NW structures is interpreted as more efficient in migrating shortening into the foreland.

An along-strike zone of ENE-NE long axes is present in both models II and III but it seems to be more localized in the western anisotropy than in model I. This zone requires a certain amount of shortening (2.5-3.0 cm) to be developed, as it was also observed for model I.

5. Discussion

5.1. Deformation patterns

Results obtained for model I (Fig. 4a-c) are similar to those obtained by Casas *et al*. (2001) for equivalent initial conditions. N-NNW long axes supporting E-ENE shortening directions together with clockwise rotations reflect dextral transpression for structures generated by reactivation of the boundaries of the silicone plate in all three models. Moreover, the slight obliquity between the NNE strained zones and the direction of shortening supports the dextral transpression. On the other hand, NNE neoformed structures show almost no rotations and are parallel to long axes of ellipses, so they can be interpreted as genuine thrusts.

The absence of significant dip-slip displacements and the presence of counterclockwise rotations on WNW reactivated structures can be interpreted as the result of dominant sinistral strike-slip displacements in model II (Fig. 5). Deformation associated with WNW structures (Fig. 5m-o) appears once the model arises a certain amount of shortening (~3 cm). This implies that these structures overprint to the previous NNE ones and control late development of some of them. Likewise, the presence of these oblique structures gives rise to along-strike segmentation of NNE structures (Fig. 5k-l).

Model III shows similarities to models I and II but a much more significant component of dip-slip displacement in the NW structures (Fig. 6) revealed by high values of ellipticity and observations in cross-sections. Together with counterclockwise rotations, these results point out to sinistral reverse-slip motions for the NW structures.

If all three models are considered, it can be observed that oblique WNW-NW structures are not developed (model I) if there is not an inherited fabric of similar orientation that can be reactivated (models II and III). These results are consistent with several proposals (Flinch and Casas, 1996; Pohn, 2001; Japas *et al*., 2010; Oriolo, 2012; Oriolo *et al*., 2013) where

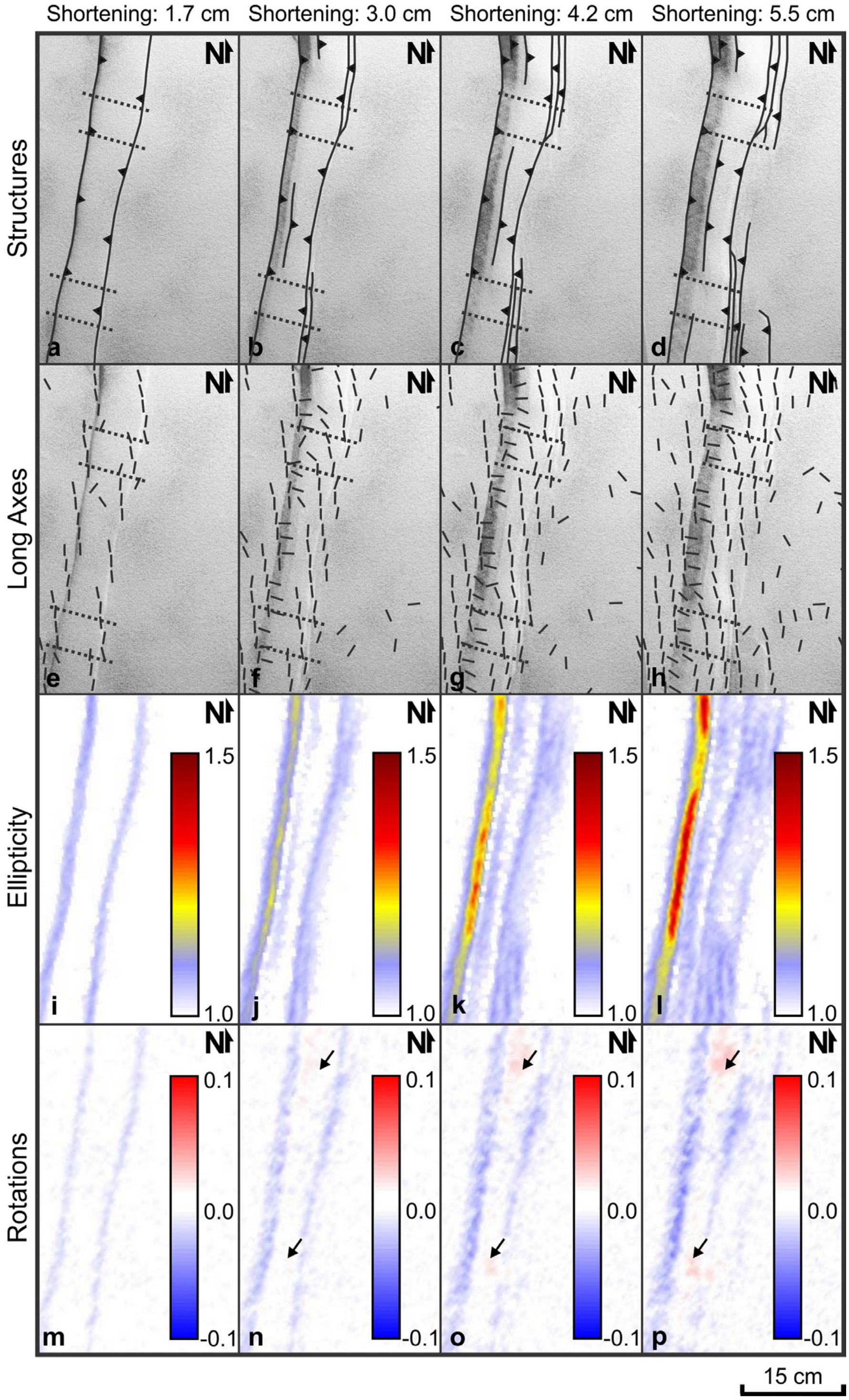

FIG. 5. Deformation stages of model II, considering main structures (**a-d**), long axes of finite strain ellipses (**e-h**), ellipticity (**i-l**) and rotations (**m-p**). Dotted lines show position of the basal WNW anisotropies. Values of ellipticity and rotations (negative rotations, clockwise; positive rotations, counterclockwise) are shown in lateral bars. Small arrows show areas of local counterclockwise rotations.

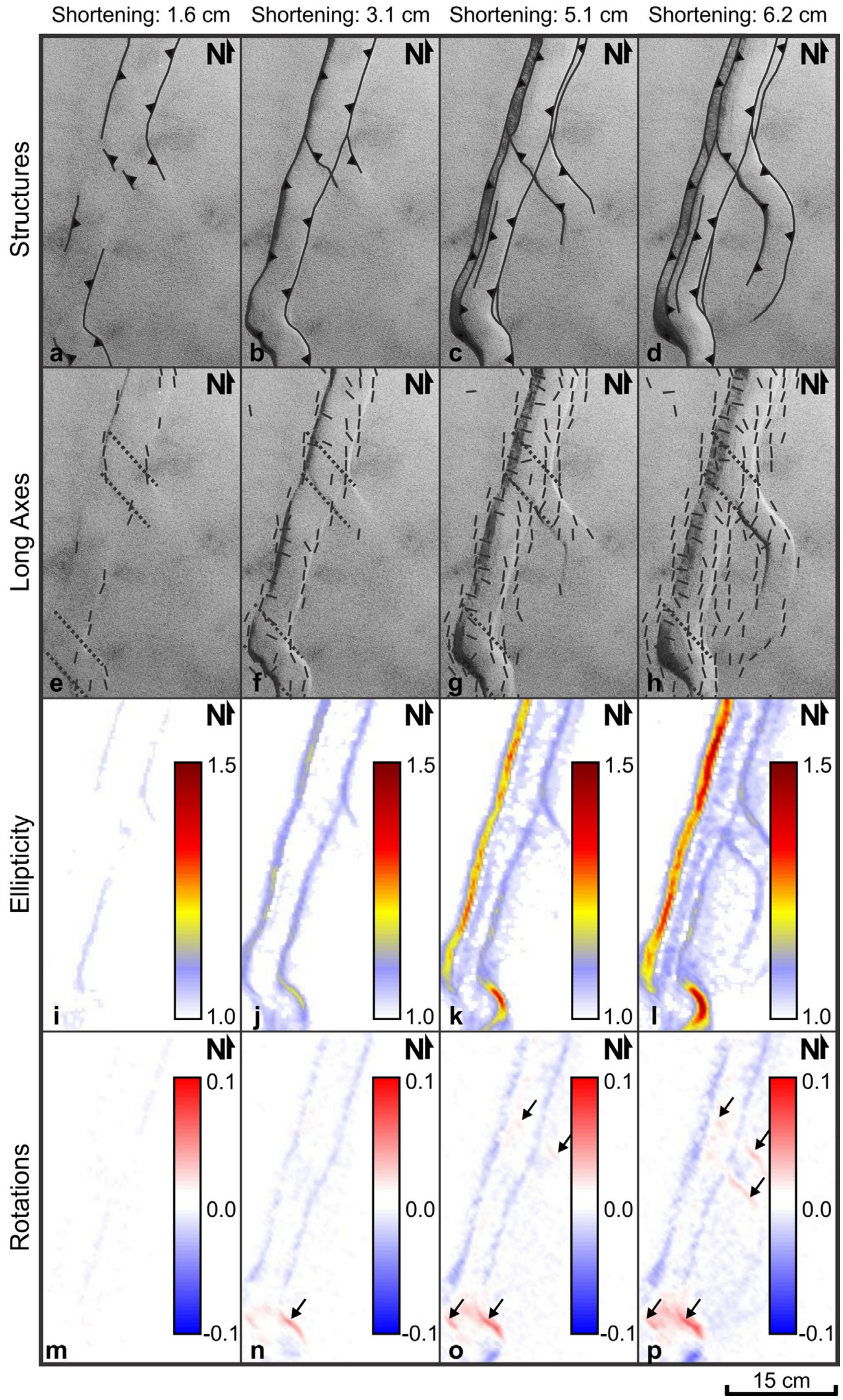

FIG. 6. Deformation stages of model III, considering main structures (**a-d**), long axes of finite strain ellipses (**e-h**), ellipticity (**i-l**) and rotations (**m-p**). Dotted lines show position of the basal NW anisotropies. Values of ellipticity and rotations (negative rotations, clockwise; positive rotations, counterclockwise) are shown in lateral bars. Small arrows show areas of local counterclockwise rotations.

cross-strike structures are described as pre-existing crustal fabrics. Moreover, similar geometrical and kinematical relationships between dextral shear zones and secondary oblique sinistral ones were presented by theoretical models of Jiang (1994) and examples from the Zagros fold and thrust belt (Hessami *et al*., 2001), the Atacama fault system (Cembrano *et al*., 2005) and the Cap de Creus (Carreras *et al*., 2013). However, oblique ENE-trending structures do develop even though previous structures are not present (Fig. 4i).

The along-strike zone with WNW-NW long axes of ellipses is clearly developed in all models. It is present only over the western margin in models II and III whereas it is wider in model I. The presence of this zone seems to be independent from ellipticity as it is always located in the western structure, which has lower ellipticity than the eastern one in model I but higher in models II and III. Likewise, it requires a certain amount of shortening to be developed that fits with the step when deformation from western and eastern structures start to overlap. This 2D distribution of strain axes could be explained either by WNW extension or NNE shortening. A WNW direction of extension could result from local extension of the hanging-wall such as described by Bonini *et al.* (2000). This mechanism would give rise to strike-parallel extension that would explain this pattern. However, cross-sections do not reveal extension in all models. Then, a NNE shortening direction is likely to be a most suitable interpretation that can be explained considering interference patterns. As this zone is developed due to interference patterns generated by overlapping of deformation from western and eastern structures, it would probably represent local areas of strain interference patterns that are progressively modified by regional dextral transpression.

Results and interpretations presented in this paper point out to a two-stage evolution model associated with heterogeneous strain partitioning. Three domains 1, 2 and 3 are considered to explain this model (Fig. 7). In the first stage (shortening lower than 2.5-3.0 cm), domains 1 and 2 (western and eastern structures, respectively) would represent areas of transpression, whereas domain 3 (areas of neoformed thrusts) is related to compression due to E-ENE shortening. In the second stage (shortening higher than 2.5-3.0 cm), domain 1 not only shows dextral transpression but also local interference patterns. Likewise, domains 2 and 3 behave as in the first stage. WNW sinistral cross-strike structures activate during this stage suggesting that they could be related to the change in deformation patterns in domain 1.

The experiments presented herein agree with Jones *et al.* (1997) about a partitioned transpressional system with strike-slip components of deformation localized in narrow zones and broader areas of relative coaxial shortening. However, this proposal shows a much more complex pattern of strain partitioning than the classical model from Tikoff and Teyssier (1994). This would be explained due to the presence of pre-existing structures in the silicone layer, whose margins are also slightly oblique to the regional shortening direction. In agreement with Carreras *et al*. (2013), the existence of structural weaknesses gives rise to complex patterns of strain partitioning, which is favored by their presence (Dewey *et al*. 1998). In addition, the observed localization of strike-slip components in the reactivated structures matches ideas of Lister and Williams (1983), which proposed that non-coaxial flow is favored by suitably oriented inherited structures.

5.2. Models and the Neogene structure of the Precordillera

Dextral transpression obtained in models by the presence of N-NNE thrusts and clockwise rotations are consistent with proposals from Siame *et al.* (2005) and Álvarez Marrón *et al.* (2006) for the Precordillera. Particularly, strain partitioning into areas dominated by dextral oblique-slip or dip-slip displacements obtained in simulations presented herein supports the hypothesis of Siame *et al*. (2005). Within this framework, domain 1 would be equivalent to the dextral strike-slip El Tigre fault (Bastías *et al*., 1984; Siame *et al*., 1997; Cortés *et al*., 1999) located in the western margin of the Precordillera (Fig. 7a, b). Differences between transpression obtained in models and dominant strike-slip displacements recorded on the El Tigre fault could be explained due to kinematic changes in the later, as some authors have suggested (Fazzito, 2011; Fazzito *et al*., 2011). However, Álvarez Marrón *et al*. (2006) described a positive flower structure developed as the result of transpression in the Iglesia basin, located immediately to the north of the El Tigre fault, which would match better the kinematics observed in the models. Neoformed

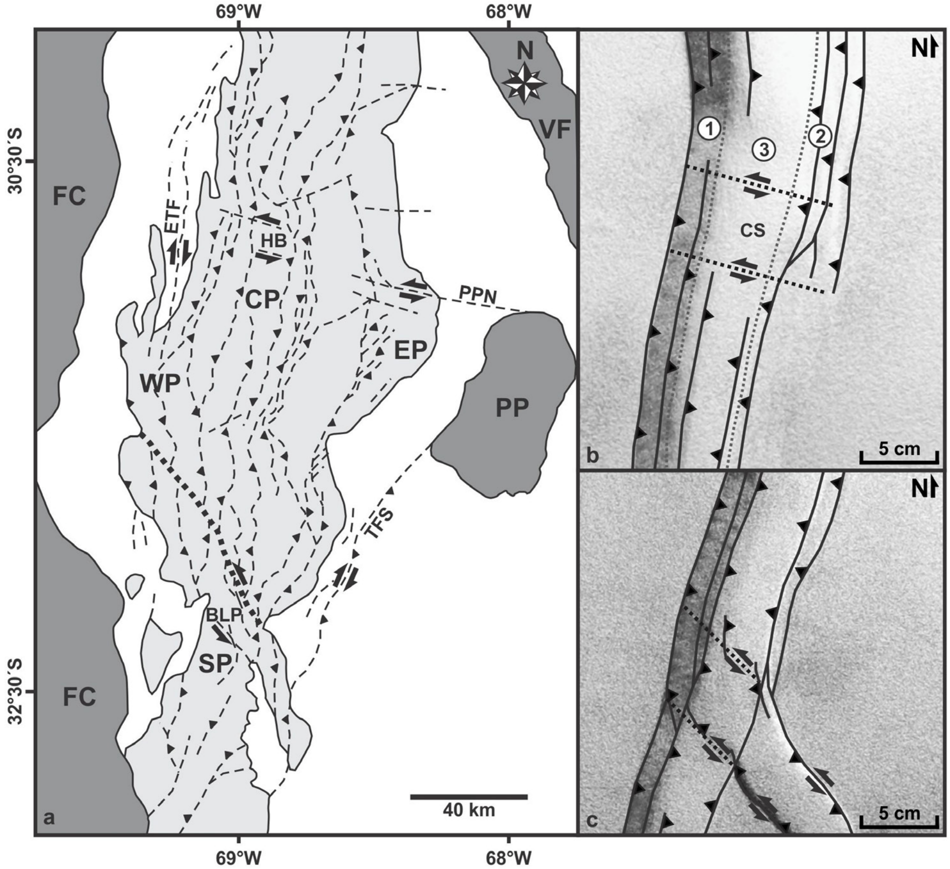

FIG. 7. Comparison of the structure of the Precordillera and analogue models. **a**. Structural map of the Precordillera (modified from Fig. 2); **b**. Model II (modified from Fig. 5d) showing the main structural features comparable to the northern Precordillera. Domains 1, 2 and 3 as well as sinistral WNW structures equivalent to the Hualilán belt are shown; **c**. Model III (modified from Fig. 6d) showing the main structural features comparable to the southern Precordillera. Sinistral reverse-slip structures equivalent to those present in the southern Precordillera are indicated.

thrusts from domain 3 would be the analogous of the Precordillera fold and thrust belt (Allmendinger *et al*., 1990; Cristallini and Ramos, 2000) whereas domain 2 would be equivalent to the Tulum fault system (Fig. 7a, b), where both reverse and dextral-strike slip deformation have been recently registered (Perucca and Ruiz, 2014). Furthermore, these equivalences allow interpreting that the oblique-slip displacements may result from reactivation of preexisting basement structures that correspond to Paleozoic terrane boundaries (Giménez *et al*., 2008; Perucca and Ruiz, 2014).

Minor differences between models and data from the Precordillera could be explained considering the complexity of the strain partitioning processes (Jones and Tanner, 1995; Chemenda *et al*., 2000) that were not considered in the analogue models. In addition, the lack of a wide database of kinematic indicators in the Precordillera faults avoids carrying out more detailed analysis and comparisons.

Regional E-ENE shortening directions obtained by strain patterns from the models are similar to those obtained for the Precordillera by Siame *et al*. (2005) on the basis of kinematic data. Clockwise rotations observed in the models are related to dextral transpression and are comparable to paleomagnetic data from Japas and Ré (2012) and Vizán *et al*. (2013). Likewise, these clockwise rotations are equivalent to rotations of kinematic axes (Siame *et al*., 2005; Oriolo *et al*., 2013) within the Precordillera. These rotations around vertical axes could be also explained by changes in the direction of convergence between the Nazca and South America plates. However, Somoza and Ghidella (2005) have provided data that supports a rather constant direction of convergence during the last 26 My.

Comparison between analogue models and structural and geophysical data from the Hualilán area (Oriolo, 2012; Oriolo *et al*., 2013) suggests that model II is the best analogue of cross-strike structures in the Precordillera (Fig. 7a, b). Strain axes and rotations obtained in model II reflect dominant sinistral strike-slip motions and are also similar to those obtained through kinematic indicators in the Hualilán belt by Oriolo (2012) and Oriolo *et al*. (2013). Moreover, temporal relationships are equivalent (cross-strike structures postdating regional thrusting) in both model and field data. The Hualilán belt would be related to the Pie de Palo Norte lineament (Fig. 2; Oriolo *et al*., 2013), which also shows equivalent geometry and kinematics to those observed in the models (Zapata, 1998). The Pie de Palo Norte lineament was considered to be the boundary of a Mesozoic rift basin (Martínez and Colombi, 2011), indicating a pre-Neogene age for this structure. Similar relationships have been also reported in the northernmost Precordillera (~29º45'S) by Chernicoff and Nash (2002). These authors recognized sinistral NW structures that may represent reactivated preexistent features and cross-cut and rotate structures of the fold and thrust belt.

Model III shows similar deformation patterns with those obtained by analogue modeling of rift inversion by Yagupsky *et al*. (2008) and Yaguspky (2010). These results are both in agreement with structural data from the southern Precordillera (Fig. 7a, c), where a Cenozoic sinistral transpression has been reported due to reactivation of Paleozoic-Triassic NNW-NNE structures (Cortés *et al*., 2005, 2006; Giambiagi *et al*., 2010; Terrizzano *et al*., 2010). Particularly, the structures obtained in the models would be equivalent to the Barreal-Las Peñas belt (Fig. 7a; Terrizzano *et al*., 2010) and similar systems located therein.

The absence of WNW structures in model I supports the idea that these structures do not developed unless they represent pre-existing fabrics (models II and III). This is consistent with hypotheses that suggest NW-WNW cross-strike structures as pre-Neogene structures that were reactivated during the Miocene (Chernicoff and Nash, 2002; Oriolo, 2012; Oriolo *et al*., 2013). Different shortening rates between along-strike segments of the Precordillera could have favored the development of WNW structures as neoformed transference zones. However, all previous studies (Allmendinger *et al*., 1990; Cristallini and Ramos, 2000; Álvarez Marrón *et al*., 2006) point out to deformation and uplifting of the northern Precordillera as a single block and consequently the hypothesis of WNW neoformed structures is discarded.

5.3. Along-strike segmentation and cross-strike structures

Segmentation models suggest that faults are divided into discrete units that behave distinctively during rupture cycles (Schwartz and Coppersmith, 1986). These units are separated by segment barriers than inhibit propagation of rupture towards other segments (Aki, 1979, 1984). Several authors have applied these segmentation models mostly on single fault seismic cycles and their rupture patterns (Schwartz and Coppersmith, 1984; Mueller and Talling, 1997; Pizzi and Galadini, 2009; Lin *et al.,* 2011).

Models presented herein reveal that WNW cross-strike structures behave as persistent barriers of rupture along major NNE faults. They give rise to local bends as well as they segmentate the strain patterns (Fig. 5f-h). These results suggest that cross-strike structures not only behave as barriers of single faults ruptures as many authors have already remarked (Schwartz and Coppersmith, 1984, 1986; Pizzi and Galadini, 2009; Lin *et al*., 2011) but also develop a significant role in the evolution and construction of orogens.

6. Concluding remarks

Analogue models presented herein provide data about deformation patterns resulting from the interaction of different set of structures. Comparison between these results and structural and geophysical data from the Precordillera let to outline these main conclusions:

- NNE heterogeneities are reactivated as dextral reverse structures that accommodate both E-ENE shortening and clockwise rotations. Neoformed NNE structures are also developed as genuine thrusts. These results support partitioned dextral transpression for the northern Andean Precordillera related to a compressive regime, confirming previous proposals from Siame *et al*. (2005).

However, dextral strike-slip displacements would not be restricted to the El Tigre fault but also to the eastern margin, as the models and recently published data suggests (Perucca and Ruiz, 2014).

- WNW and NW weaknesses are reactivated as sinistral strike-slip (β=100º) or sinistral transpressional (β=130º) structures that do not develop unless they represent inherited structures. WNW structures are equivalent to those described in the northern Precordillera as they show similar orientation and kinematics and they postdate regional thrusting. NW anisotropies show similarities with Paleozoic-Triassic structures reactivated during the Andean orogeny in the southern Precordillera.
- Cross-strike structures have a major role in the segmentation of the thrust belt. Therefore, they have to be carefully considered in further works related to seismic hazards within the Precordillera, as they are probably behaving as barriers of fault rupture.

Acknowledgements

S. Oriolo thanks a 2011-2012 research grant from the Consejo Interuniversitario Nacional. E. Cristallini acknowledges projects PICT 1441 from the Agencia Nacional de Promoción Científica y Tecnológica and UBACyT 20020100100855 from the Universidad de Buenos Aires. M.S. Japas thanks project PIP 11420100100334 from the Consejo Nacional de Investigaciones Científicas y Técnicas. H. Vizán, J. Cortés and J. Sellés-Martínez (Instituto de Geociencias Básicas, Aplicadas y Ambientales, Universidad de Buenos Aires-CONICET) and L. Dimieri (Instituto Geológico del Sur, Universidad Nacional del Sur-CONICET) are acknowledged for previous discussions related to this work. The authors are indebted to the editor for the editorial work and L. Giambiagi (Instituto Argentino de Nivología, Glaciología y Ciencias Ambientales-CONICET) for the suggestions and corrections that helped to improve this manuscript.

References

Adam, J.; Urai, J.L.; Wieneke, B.; Oncken, O.; Pfeiffer, K.; Kukowski, N.; Lohrmann, J.; Hoth, S.; van der Zee, W.; Schmatz, J. 2005. Shear localisation and strain distribution during tectonic faulting-new insights from granular-flow experiments and high-resolution optical image correlation techniques. Journal of Structural Geology 27: 283-301.

Aki, K. 1979. Characterization of barriers on an earthquake fault. Journal of Geophysical Research 84: 6140-6148.

Aki, K. 1984. Asperities, barriers, characteristic earthquakes, and strong motion prediction. Journal of Geophysical Research 89: 5867-5872.

Allmendinger, R.W.; Figueroa, D.; Snyder, D.; Beer, J.; Mpodozis, C.; Isacks, B.L. 1990. Foreland shortening and crustal balancing in the Andes at 30ºS latitude. Tectonics 9 (4): 789-809.

Álvarez Marrón, J.; Rodríguez Fernández, R.; Heredia, N.; Busquets, P.; Colombo, F.; Brown, D. 2006. Neogene structures overprinting Palaeozoic thrusts systems in the Anden Precordillera at 30ºS latitude. Journal of the Geological Society of London 163: 949-964.

Anderson, M.; Alvarado, P.; Zandt, G.; Beck, S.L. 2007. Geometry and brittle deformation of the subducting Nazca Plate, central Chile and Argentina. Geophysical Journal International 171 (1): 419-434.

Bastías, H.; Weidmann, N.; Pérez, M. 1984. Dos zonas de fallamiento plio-cuaternario en la Precordillera de San Juan. *In* Congreso Geológico Argentino, No. 9, Actas 2: 329-341. San Carlos de Bariloche.

Bonini, M.; Sokoutis, D.; Mulugeta, G.; Katrivanos, E. 2000. Modeling hanging wall accommodation above rigid thrust ramps. Journal of Structural Geology 8: 1165-1179.

Brooks, B.A.; Bevis, M.; Smalley, R.; Kendrick, E.; Manceda, R.; Lauría, E.; Maturana, R.; Araujo, M. 2003. Crustal motion in the Southern Andes (26º-36ºS): Do the Andes behave like a microplate? Geochemistry, Geophysics, Geosystems 4 (10) , 1085. doi: 10.1029/2003GC000505.

Carreras, J.; Cosgrove, J.W.; Druguet, E. 2013. Strain partitioning and/or anisotropic rocks: Implications for inferring tectonic regimes. Journal of Structural Geology 50: 7-21.

Casas, A.M.; Gapais, D.; Nalpas, T.; Besnard, K.; Román-Berdiel, T. 2001. Analogue models of transpressive systems. Journal of Structural Geology 5: 733-743.

Casassa, E.Z.; Sarquis, A.M.; Van Dyke, C.H. 1986. The gelation of polyvinyl alcohol with borax: a novel class participation experiment involving the preparation and properties of a "slime". Journal of Chemical Education 63 (1): 57-60.

Cembrano, J.; González, G.; Arancibia, G.; Ahumada, I.; Olivares, V.; Herrera, V. 2005. Fault zone development and strain partitioning in an extensional strike-slip duplex: A case study from the Mesozoic Atacama fault system, Northern Chile. Tectonophysics 400: 105-125.

Chemenda, A.; Lallemand, S.; Bokun, A. 2000. Strain partitioning and interplate friction in oblique subduction zones. Journal of Geophysical Research 105 (B3): 5567-5581.

Chernicoff, C.J.; Nash, C.R. 2002. Geological interpretation of Landsat TM imagery and aeromagnetic survey data, northern Precordillera region, Argentina. Journal of South American Earth Sciences 14 (8): 813-820.

Cloos, H. 1928. Experimenten zur inneren Tektonik. Zentralblatt für Mineralogie Paläontologie 1928B: 609-621.

Cortés, J.M.; Vinciguerra, P.; Yamín, M.; Pasini, M.M. 1999. Tectónica Cuaternaria de la Región Andina del Nuevo Cuyo (28°-33º LS). *In* Geología Argentina (Caminos, R.; editor). Anales del Instituto de Geología y Recursos Minerales: 760-778. Buenos Aires.

Cortés, J.M.; Pasini, M.; Yamín, M. 2005. Paleotectonic controls on the distribution of Quaternary deformation in the southern Precordillera, Central Andes (31º30'-33º sl). *In* International Symposium on Andean Geodynamics, No. 6, Extended Abstracts: 186-189. Barcelona.

Cortés, J.M.; Casa, A.; Pasini, M.; Yamín, M.; Terrizzano, C.M. 2006. Fajas oblicuas de deformación neotectónica en Precordillera y Cordillera Frontal (31º30'-33º30' ls): controles paleotectónicos. Revista de la Asociación Geológica Argentina 61 (4): 639-646.

Corti, G.; Moratti, G.; Sani, F. 2005. Relations between surface faulting and granite intrusions in analogue models of strike-slip deformation. Journal of Structural Geology 27: 1547-1562.

Cristallini, E.O.; Ramos, V.A. 2000. Thick-skinned and thin-skinned thrusting in La Ramada fold and thrust belt: Crustal evolution of the High Andes of San Juan, Argentina (32°SL). Tectonophysics 317: 205-235.

Davy, P.; Cobbold, P.R. 1991. Experiments on shortening of a 4-layer model of the continental lithosphere. Tectonophysics 188 (1-2): 1-25.

Dewey, J.F.; Holdsworth, R.E.; Strachan, R.E. 1998. Transpression and transtension zones. *In* Continental transpressional and transtensional tectonics (Holdsworth, R.E.; Strachan, R.E.; Dewey, J.F.; editors). Geological Society of London, Special Publications 135: 1-14. London.

Dooley, T.; McClay, K. 1997. Analog modeling of pull-apart basins. American Association of Petroleum Geologists Bulletin 81: 1804-1826.

Fazzito, S.Y. 2011. Estudios geofísicos aplicados a la neotectónica de la falla El Tigre, Precordillera de San Juan. Ph.D. Thesis (Unpublished), Universidad de Buenos Aires: 260 p.

Fazzito, S.Y.; Rapalini, A.E.; Cortés, J.M.; Terrizzano, C.M. 2011. Kinematic study in the area of the Quaternary El Tigre fault, Western Precordillera, Argentina on the basis of paleomagnetism and anisotropy of magnetic susceptibility. Latinmag Letters 1 (2): B24: 1-5.

Flinch, J.F.; Casas, J.M. 1996. Inversion of a transfer system into lateral ramps: An example from the South-Central Pyrenees (Spain). Geologische Rundschau 85 (2): 372-379.

Giambiagi, L.; Mescua, J.; Bechis, F.; Martínez, A.; Folguera, A. 2010. Pre-Andean deformation of the Precordillera southern sector, southern Central Andes. Geosphere 7 (1): 219-239.

Giménez, M.E.; Martínez, P.M.; Introcaso, A. 2008. Lineamientos regionales del basamento cristalino a partir de un análisis gravimétrico. Revista de la Asociación Geológica Argentina 63 (2): 288-296.

Hessami, K.; Koyi, H.A.; Talbot, C.J. 2001. The significance of strike-slip faulting in the basement of the Zagros fold and thrust belt. Journal of Petroleum Geology 24 (1): 5-28.

Japas, M.S. 1998. Aporte del análisis de fábrica deformacional al estudio de la faja orogénica andina. Homenaje al Dr. Arturo J. Amos. Revista de la Asociación Geológica Argentina 53 (1): 15.

Japas, M.S.; Ré, G.H. 2012. Neogene tectonic block rotations and margin curvature at the Pampean flat slab segment (28º-33º SL, Argentina). Geoacta 37 (1): 1-4.

Japas, M.S.; Ré, G.H.; Barredo, S.P. 2002a. Lineamientos andinos oblicuos (entre 22° y 33°S): definidos a partir de fábricas tectónicas. I. Fábrica deformacional y de sismicidad. *In* Congreso Geológico Argentino, No. 15, Actas 1: 326-331. El Calafate.

Japas, M.S.; Ré, G.H.; Barredo, S.P. 2002b. Lineamientos andinos oblicuos (entre 22° y 33°S) definidos a partir de fábricas tectónicas. III. Modelo cinemático. *In* Congreso Geológico Argentino, No. 15, Actas 1: 340-343. El Calafate.

Japas, M.S.; Urbina, N.E.; Sruoga, P. 2010. Control estructural en el emplazamiento del volcanismo y mineralizaciones neógenas, distrito Cañada Honda, San Luis. Revista de la Asociación Geológica Argentina 67 (4): 494-506.

Jiang, D. 1994. Vorticity determination, distribution, partitioning and the heterogeneity and non-steadiness of natural deformations. Journal of Structural Geology 16 (1): 121-130.

Jones, R.R.; Tanner, P.W.G. 1995. Strain partitioning in transpression zones. Journal of Structural Geology 17 (6): 793-802.

Jones, R.R.; Holdsworth, R.E.; Bailey, W. 1997. Lateral extrusion in transpression zones: the importance of boundary conditions. Journal of Structural Geology 19 (9): 1201-1217.

Jordan, T.E.; Allmendinger, R.W.; Damanti, T.; Drake, R.E. 1993. Chronology of motion in a complete thrust belt: the Precordillera, 30-31°S, Andes Mountains. Journal of Geology 101: 135-156.

Kay, S.M.; Maksaev, V.; Moscoso, R.; Mpodozis, C.; Nasi, C. 1987. Probing the evolving Andean lithosphere: mid-late Tertiary magmatism in Chile (29-30º30'S) over the modern zone of subhorizontal subduction. Journal of Geophysical Research 92 (7): 6173-6189.

Le Guerroué, E.; Cobbold, P.R. 2006. Influence of erosion and sedimentation on strike-slip fault systems: insights from analogue models. Journal of Structural Geology 28 (3): 421-430.

Leever, K.A.; Gabrielsen, R.H.; Sokoutis, D.; Willingshofer, E. 2011. The effect of convergence angle on the kinematic evolution of strain partitioning in transpressional brittle wedges: Insight from analog modelling and high-resolution digital image analysis. Tectonics 30, TC2013. doi: 10.1029/2010TC002823.

Likerman, J.; Burlando, J.F.; Cristallini, E.O.; Ghiglione, M.C. 2013. Along-strike structural variations in the Southern Patagonian Andes: Insights from physical modeling. Tectonophysics 590: 106-120.

Lin, J.; Stein, R.S.; Meghraoui, R.; Toda, S.; Ayadi, A.; Dorbath, C.; Belabbes, S. 2011. Stress transfer among en echelon and opposing thrusts and tear faults: Triggering caused by the 2003 Mw=6.9 Zemmouri, Algeria, earthquake. Journal of Geophysical Research 116, B03055. doi: 10.1029/2010JB007654.

Lister, G.S.; Williams, P.F. 1983. The partitioning of deformation in rock masses. Tectonophysics 92: 1-33.

Martínez, R.N.; Colombi, C.E. 2011. Evolución litofacial y edad de la Formación Cañón del Colorado. Revista de la Asociación Geológica Argentina 68 (1): 96-108.

Mathieu, L.; van Wyk de Vries, B. 2011. The impact of strike-slip, transtensional and transpressional fault zones on volcanoes. Part 1: Scaled experiments. Journal of Structural Geology 33 (5): 907-917.

Mathieu, L.; van Wyk de Vries, B.; Pilato, M.; Troll, V.R. 2011. The interaction between volcanoes and strike-slip, transtensional and transpressional fault zones: Analogue models and natural examples. Journal of Structural Geology 33 (5): 898-906.

Mueller, K.; Talling, P. 1997. Geomorphic evidence of tear faults accommodating lateral propagation of and active fault-bend fold, Wheeler Ridge, California. Journal of Structural Geology 19 (3-4): 397-411.

Oriolo, S. 2012. Análisis de la deformación en la región de Hualilán, Precordillera de San Juan. Trabajo Final de Licenciatura (Unpublished), Universidad de Buenos Aires, Facultad de Ciencias Exactas y Naturales: 160 p.

Oriolo, S.; Japas, M.S.; Cristallini, E.O.; Giménez, M. 2013. Cross-strike structures controlling magmatism emplacement in a flat-slab setting (Precordillera, Central Andes of Argentina). *In* Deformation Structures and Processes within the Continental Crust (Llana-Fúnez, S.; Marcos, A.; Bastida, F.; editors). Geological Society of London, Special Publications 394. doi:10.1144/SP394.6. London.

Perucca, L.; Ruiz, F. 2014. New data on neotectonic contractional structures in Precordillera, south of Río de la Flecha: Structural setting addressed by gravimetry and magnetic data. San Juan, Argentina. Journal of South American Earth Sciences 50: 1-11.

Pilger, R.H. 1984. Cenozoic plate kinematics, subduction and magmatism: South American Andes. Journal of the Geological Society of London 141: 793-802.

Pinnet, N.; Cobbold, P.R. 1992. Experimental insights into the partitioning of motion within zones of oblique subduction. Tectonophysics 206 (3-4): 371-388.

Pizzi, A.; Galadini, F. 2009. Pre-existing cross-structures and active fault segmentation in the northern-central Apennines (Italy). Tectonophysics 476: 304-319.

Pohn, H.A. 2001. Lateral ramps in the folded Apalaches and in overthrust belts overwide-A fundamental element of thrust-belt architecture. U.S. Geological Survey Bulletin 2163: 71 p. Denver.

Rahe, B.; Ferrill, D.A.; Morris, A.P. 1998. Physical analog modeling of pull-apart basin evolution. Tectonophysics 285 (1-2): 21-40.

Ramos, V.A. 1999a. Plate tectonic setting of the Andean Cordillera. Episodes 22 (3): 183-190.

Ramos, V.A. 1999b. Las provincias geológicas del territorio argentino. *In* Geología Argentina (Caminos, R.; editor). Anales del Instituto de Geología y Recursos Minerales 41-96. Buenos Aires.

Ramos, V.A.; Cristallini, E.O.; Pérez, D.J. 2002. The Pampean flat-slab of the Central Andes. Journal of South American Earth Sciences 15: 59-78.

Ré, G.H.; Japas, M.S. 2004. Andean oblique megashear zones: paleomagnetism contribution. Geological Society of America Abstract with Programs, 36, Abstract No. 79033.

Ré, G.H.; Japas, M.S.; Barredo, S.P. 2000. Análisis de fábrica deformacional (AFD): el concepto fractal cualitativo aplicado a la definición de lineamientos cinemáticos neógenos en el noroeste argentino. *In* Reunión sobre Microtectónica, No. 10, Resúmenes: 12. Buenos Aires.

Ré, G.H.; Japas, M.S.; Barredo, S.P. 2001. Análisis de fábrica deformacional (AFD): el concepto fractal cualitativo aplicado a la definición de lineamientos cinemáticos neógenos en el noroeste argentino. Revista de la Asociación Geológica Argentina, Publicación Especial 5: 75-82.

Richard, P.; Cobbold, P.R. 1989. Structures en fleur positives et decróchements crustaux: modélisation analoguique. Comptes Rendus de l´Académie des Sciences de Paris 308: 553-560.

Richard, P.; Cobbold, P.R. 1990. Experimental insights into partitioning of fault motions in continental convergent wrench zones. Annales Tectonicae 4: 35-44.

Riedel, W. 1929. Zur mechanik geologischer Brucherscheinungen. Zentralblatt für Mineralogie und Paläontologie 1929B: 354-368.

Schreurs, G.; Colletta, B. 1998. Analogue modeling of faulting in zones of continental transpression and transtension. *In* Continental transpressional and transtensional tectonics (Holdsworth, R.E.; Strachan, R.A.; Dewey, J.F.; editors). Geological Society of London, Special Publications 135: 59-79. London.

Schwartz, D.P.; Coppersmith, K.J. 1984. Fault behavior and characteristic earthquakes. Examples from the Wasatch and San Andreas fault zones. Journal of Geophysical Research 89: 5681-5698.

Schwartz, D.P.; Coppersmith, K.J. 1986. Seismic hazards New trends in analysis using geologic data. *In* Active tectonics Studies in geophysics (Wallace, R.E.; editor). National Academy Press: 215-230. Washington.

Siame, L.L.; Sébrier, M.; Bellier, O.; Bourlès, D.L.; Castano, J.C.; Araujo, M. 1997. Geometry, segmentation and displacement rates of the El Tigre Fault, San Juan Province (Argentina) from SPOT image analysis and 10Be datings. Annales Tectonicae 1-2: 3-26.

Siame, L.L.; Bellier, O.; Sebrier, M.; Araujo, M. 2005. Deformation partitioning in flat subduction setting: Case of the Andean foreland of western Argentina (28ºS-33ºS). Tectonics 24, TC5003. doi: 10.1029/2005TC001787.

Somoza, R.; Ghidella, M.E. 2005. Convergencia en el margen occidental de América del Sur durante el Cenozoico: subducción de las placas de Nazca, Farallón y Aluk. Revista de la Asociación Geológica Argentina 60 (4): 797-809.

Soto, R.; Martinod, J.; Odonne, F. 2007. Influence of early strike-slip deformation on subsequent perpendicular shortening: An experimental approach. Journal of Structural Geology 29: 59-72.

Stewart, L. 1996. Behaviour of spherical rigid objects and passive markers during bulk inhomogeneous shortening of a fluid. Journal of Structural Geology 18 (1): 121-130.

Sveen, J.K. 2004. An introduction to matpiv v.1.6.1. Department of Mathematics, University of Oslo. http://www.math.uio.no/~jks/matpiv. Accessed 30 October 2012.

Terrizzano, C.M.; Fazzito, S.Y.; Cortés, J.M.; Rapalini, A.E. 2010. Studies of Quaternary deformation zones through geomorphic and geophysical evidence. A case in the Precordillera Sur, Central Andes of Argentina. Tectonophysics 490: 184-196.

Tikoff, B.; Teyssier, C. 1994. Strain modeling of displacement-field partitioning in transpressional orogens. Journal of Structural Geology 16: 1575-1588.

Vizán, H.; Geuna, S.; Melchor, R.; Bellosi, E.S.; Lagorio, S.L.; Vásquez, C.; Japas, M.S.; Ré, G.; Do Campo, M. 2013. Geological setting and paleomagnetism of the Eocene red beds of Laguna Brava Formation (Quebrada Santo Domingo, northwestern Argentina). Tectonophysics 583: 105-123.

White, D.J.; Take, W.A.; Bolton, M.D. 2001. Measuring soil deformation in geotechnical models using digital images and PIV analysis. *In* International Conference on Computer Methods and Advances in Geomechanics, No. 10, Abstracts: 997-1002. Rotterdam.

Yagupsky, D.L. 2010. Metodología para el estudio de sistemas compresivos y de sus controles estucturales. Ph.D. Thesis (Unpublished), Universidad de Buenos Aires: 203 p.

Yagupsky, D.L.; Cristallini, E.O.; Fantín, J.; Zamora Valcarce, G.; Bottesi, G.; Varadé, R. 2008. Oblique half-graben inversion of the Mesozoic Neuquén Rift in the Malargüe Fold and Thrust Belt, Mendoza, Argentina: New insights from analogue models. Journal of Structural Geology 30: 839-853.

Zapata, T.R. 1998. Crustal structure of the Andean thrust front at 30°S latitude from shallow and deep seismic reflection profiles, Argentina. Journal of South American Earth Sciences 11 (2): 131-151.

Zapata, T.R.; Allmendinger, R.W. 1996. Thrust front zone of the Precordillera, Argentina: a thick skinned triangle zone. American Association of Petroleum Geologists, Bulletin 80 (3): 350-381.

Manuscript received: March 10, 2014; revised/accepted: September 29, 2014; available online: October 1, 2014.